

Organic & Biomolecular Chemistry

Accepted Manuscript



This article can be cited before page numbers have been issued, to do this please use: N. Bernardo-García, P. A. Sánchez-Murcia, A. Espailat, C. S. Martínez-Caballero, F. Cava, J. Hermoso and F. Gago, *Org. Biomol. Chem.*, 2019, DOI: 10.1039/C9OB00223E.



This is an Accepted Manuscript, which has been through the Royal Society of Chemistry peer review process and has been accepted for publication.

Accepted Manuscripts are published online shortly after acceptance, before technical editing, formatting and proof reading. Using this free service, authors can make their results available to the community, in citable form, before we publish the edited article. We will replace this Accepted Manuscript with the edited and formatted Advance Article as soon as it is available.

You can find more information about Accepted Manuscripts in the [author guidelines](#).

Please note that technical editing may introduce minor changes to the text and/or graphics, which may alter content. The journal's standard [Terms & Conditions](#) and the ethical guidelines, outlined in our [author and reviewer resource centre](#), still apply. In no event shall the Royal Society of Chemistry be held responsible for any errors or omissions in this Accepted Manuscript or any consequences arising from the use of any information it contains.

Cold-induced aldimine bond cleavage by Tris in *Bacillus subtilis* alanine racemase[†]

Noelia Bernardo-García^a, Pedro A. Sánchez-Murcia^b, Akbar Espaillet^c, Siseth Martínez-Caballero^a,
Felipe Cava^c, Juan A. Hermoso^{*a}, and Federico Gago^{*b}

^a Department of Crystallography and Structural Biology, Institute of Physical Chemistry "Rocasolano", CSIC, 28006 Madrid, Spain

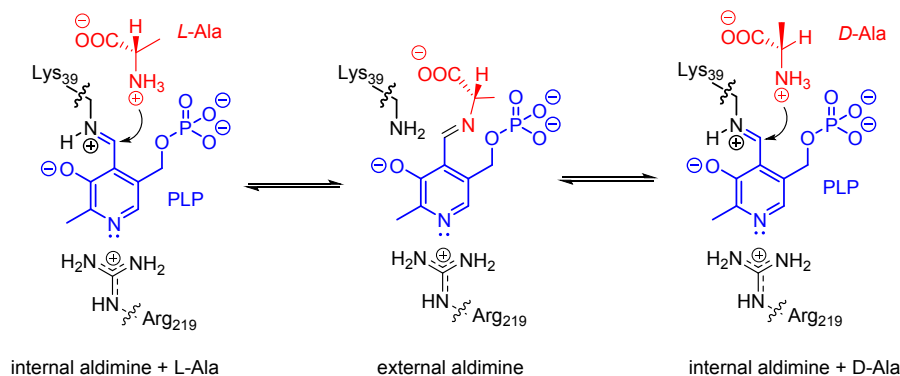
^b Department of Biomedical Sciences, "Unidad Asociada IQM-CSIC", University of Alcalá, E-28871 Alcalá de Henares, Madrid, Spain

^c Laboratory for Molecular Infection Medicine, Department of Molecular Biology, Umeå Centre for Microbial Research, Umeå University, 90187 Umeå, Sweden

*Corresponding authors. Email: xjuan@iqfr.csic.es / Email: federico.gago@uah.es

Pyridoxal 5'-phosphate (PLP) is a versatile cofactor involved in a large variety of enzymatic processes. Most of PLP-catalysed reactions, such as those of alanine racemases (AlaRs), present a common resting state in which the PLP is covalently bound to an active-site lysine to form an internal aldimine. The crystal structure of *Bs*AlaR grown in the presence of Tris lacks this covalent linkage and the PLP cofactor appears deformed. However, loss of activity in a Tris buffer only occurred after the solution was frozen prior to carrying out the enzymatic assay. This evidence strongly suggests that Tris can access the active site at subzero temperatures and behave as an alternate racemase substrate leading to mechanism-based enzyme inactivation, a hypothesis that is supported by additional X-ray structures and theoretical results from QM/MM calculations. Taken together, our findings highlight a possibly underappreciated role for a common buffer component widely used in biochemical and biophysical experiments.

Alanine racemases (AlaRs) belong to a family of homodimeric enzymes that catalyse the interconversion between L-amino acids and D-amino acids.¹ They are dependent on the coenzyme pyridoxal 5'-phosphate (PLP),² the biologically active form of vitamin B₆. AlaRs are considered promising antibacterial targets for structure-based drug design.³ In the substrate-free form, the aldehyde group of PLP forms an internal aldimine with the ε-amino group of an active-site lysine (Scheme 1). When L-Ala binds as a substrate in one monomer, its amino group undergoes a transaldimination reaction to yield an external aldimine from which the α-proton is abstracted by a tyrosine residue from the other monomer. The trigonal planar carbanion intermediate is reprotonated by the amino group of the same catalytic lysine. As a result, there is an inversion of absolute configuration at the C_α so that, when a second imine exchange reconstitutes the native form of the enzyme, D-Ala is produced and released from the active site (Scheme 1).



Scheme 1. *Bs*AlaR catalyses the racemization of L-Ala.¹

As part of our ongoing efforts to understand the structural basis for the specificity of amino acid racemases,⁴ we recently solved several crystal structures of AlaR Bsu17640 from *Bacillus subtilis* (*BsAlaR*) (**Table 1**). In common with other AlaRs, *BsAlaR* folds as a globular homodimeric enzyme and residues from both monomers make up the active site. Unexpectedly, however, we found that, in the structure crystallized in the presence of tris(hydroxymethyl)-amino-methane (Tris) at 2.1 Å resolution, the PLP is not bonded to Lys39 and Lys39' in both active sites, and the C4' atom of this cofactor is actually missing (**Figure 1**). Because of this, the enzyme reconstituted from the crystal is inactive for the catalytic transaldimination reaction in the absence of fresh PLP.

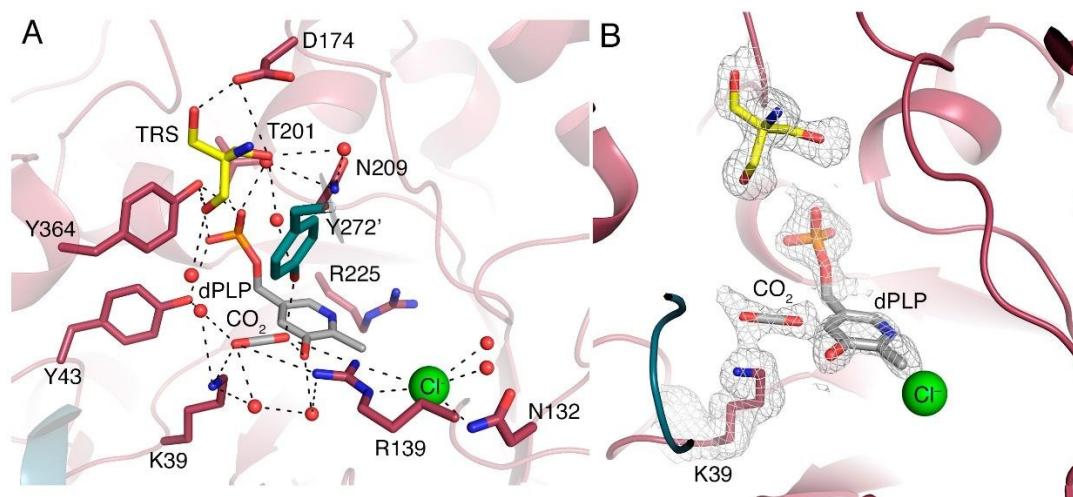


Figure 1. (A) Detail of the PLP environment within one of the active sites of *BsAlaR* co-crystallized in the presence of Tris. Relevant residues involved in the catalytic mechanism, 4'-deformyl-PLP, Tris (yellow), and CO₂ are displayed as sticks (including Tyr272' from the other subunit); water oxygens and the chloride ion are shown as red and green spheres, respectively. Hydrogen bonding interactions are indicated by dotted lines. (B) Electron density (2F_o-F_c map contoured at 1σ for 4'-deformyl-PLP, Tris, CO₂ and Lys39.

Remarkably, the racemase activity of *BsAlaR* in Tris buffer did not decrease (**Figure 2**) unless the sample was frozen before the enzymatic assay. The phenomenon of cold scission or cold lability, often influenced by pH and ionic strength,⁵ has been previously observed in a number of PLP-containing oligomeric enzymes, most notably in tetrameric *Escherichia coli* tryptophanase in buffers containing either 100 mM potassium phosphate or 100 mM KCl-50 mM tricine (*N*-[2-hydroxy-1,1-bis(hydroxymethyl)-ethyl]-glycine).⁶⁻⁸ For this enzyme, the observed aldimine bond cleavage at 2 °C is preceded by conformational changes proposed to result from the weakening of hydrophobic interactions⁵ that lead to dissociation into dimers and a reversible loss of activity. Of note, the same homotetrameric enzyme from *Proteus vulgaris*,⁹ under the same conditions, dissociates into monomers.^{6, 8}

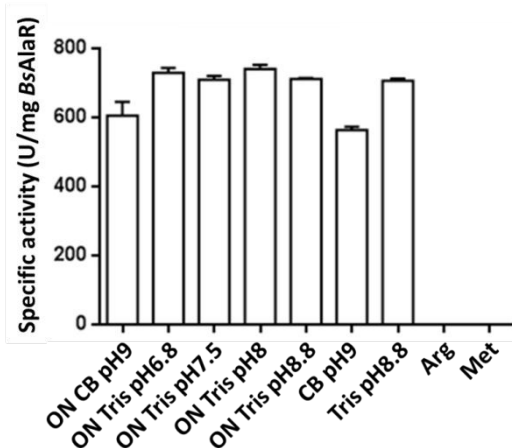


Figure 2. Specific activities (U/mg) of *BsAlaR* after incubation in 100 mM Tris at different pH values at room temperature for 30 s. Arg and Met were used as negative controls for selectivity. CB and ON stand for carbonate-bicarbonate buffer and overnight, respectively.

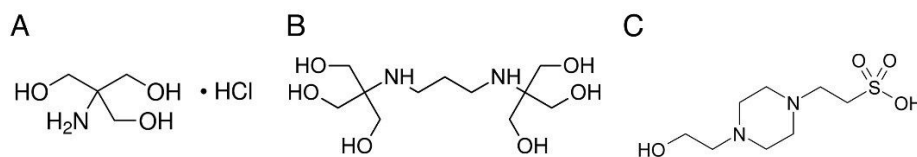


Figure 3. Chemical structures of the different buffers used for the crystallization, (A) Tris-HCl, (B) Bis-Tris propane, and (C) HEPES.

To assess whether the observed effect was specific to Tris, crystals of *BsAlaR* were also grown in the absence of buffer or at pH 8.5 in the presence of either bis-Tris propane or HEPES (**Figure 3**). These crystals were also flash cooled prior to X-ray data collection (**Table 1**) but no PLP inactivation/degradation was observed (**Figure 4**). Thus, the existence of an intact internal aldimine in these other crystal forms rules out the effect of pH and/or radiation damage on the bond cleavage detected in the presence of Tris. For the sake of reproducibility, we produced fresh protein and grew new crystals of *Bs-AlaR* by the microbatch method in a medium containing 15% PEG 4000, 0.2 M MgCl₂, 0.1 M Tris pH = 8.5 many months later; the same results were found (**Figure S1** in ESI). With the key role of Tris firmly established, we then checked several other structures of homodimeric PLP-containing enzymes solved by X-ray crystallography in the presence of Tris available in the PDB. In the following cases the 4'-aldehyde of the PLP cofactor is not covalently linked to the ϵ -amino group of the active-site lysine: (i) human KAT (*hKAT*, PDB entry 3FVX),¹⁰ (ii) human mitochondrial branched-chain aminotransferase (*hBCATm*, PDB entry 1EKV),¹¹ *E. coli* tryptophanase (PDB entry 4UP2),¹² and (iii) *Toxoplasma gondii* ornithine aminotransferase (*TgOAT*, PDB entry 5EQC).¹³ An intact Tris molecule in the active site is observed only in 5EQC whereas 1EKV reveals partial occupancy of PLP and the presence of a poorly defined reaction intermediate that was assumed to be a Tris molecule covalently bridging PLP and the active-site lysine.¹¹

Table 1. Crystallographic data collection and refinement statistics.*

| | <i>BsAlaR</i> -TRS | <i>BsAlaR</i> -nobuff | <i>BsAlaR</i> -TRSprop | <i>BsAlaR</i> -HEPES |
|--|----------------------|-----------------------|------------------------|----------------------|
| Data collection | | | | |
| Wavelength (Å) | 0.980110 | 0.979260 | 0.979340 | 0.979340 |
| Space group | P4 ₃ 22 | P2 ₁ | P4 ₃ 22 | P4 ₃ 22 |
| Unit cell <i>a, b, c</i> (Å) | 72.89, 72.89, 332.83 | 88.43, 110.53, 88.51 | 73.24, 73.24, 333.53 | 73.66, 73.66, 331.61 |
| Unit cell α, β, γ (°) | 90, 90, 90 | 90, 116.42, 90 | 90, 90, 90 | 90, 90, 90 |
| T (K) | 100 | 100 | 100 | 100 |
| X-ray source | Synchrotron | Synchrotron | Synchrotron | Synchrotron |
| Resolution range (Å) | 49.2-(2.22 -2.10) | 46.6-(2.99-2.85) | 49.6-(2.00-1.92) | 49.3-(2.05 -2.11) |
| Unique reflections | 53961 | 35532 | 70977 | 58818 |
| Completeness (%) | 100.0 (100.0) | 99.5 (99.8) | 100.0 (100.0) | 99.9(100) |
| Redundancy | 11.4 (10.2) | 3.2 (3.2) | 12.9 (12) | 16.5 (17.6) |
| R _{merge} | 0.10 (0.55) | 0.048 (1.02) | 0.05 (1.07) | 0.10 (1.26) |
| R _{pim} | 0.11 (0.35) | 0.10 (0.78) | 0.04 (0.48) | 0.05 (0.31) |
| Average <i>I</i> / σ (<i>I</i>) | 21.5 (4.8) | 5.7 (1.0) | 16.6 (2.3) | 10.1 (2.1) |
| Refinement | | | | |
| Resolution range (Å) | 49.2-2.1 | 45.3-3.0 | 49.3-1.95 | 49.3-2.05 |
| R _{work} /R _{free} | 0.16/0.20 | 0.23/0.29 | 0.20/ 0.23 | 0.19/0.24 |
| No. Atoms | | | | |
| Protein | 6033 | 12106 | 6062 | 6064 |
| Water | 538 | 7 | 571 | 345 |
| Ligand | 104 | 4 | 11 | 4 |
| B-factor (Å²) | | | | |
| Protein | 31.12 | 72.40 | 46.62 | 30.79 |
| Water | 32.5 | 63.65 | 45.80 | 42.78 |
| Ligand | 60.57 | 82.52 | 53.59 | 51.76 |
| R.m.s. deviations | | | | |
| Bond length (Å) | 0.016 | 0.015 | 0.018 | 0.025 |
| Bond angles (°) | 1.48 | 1.55 | 1.67 | 2.376 |
| Ramachandran | | | | |
| Favored/outliers (%) | 96.75/0.0 | 95.96/0.26 | 96.74/ 0.13 | 97/0.0 |
| Monomers per AU | 2 | 4 | 2 | 2 |
| PDB code | 5IRP | 6Q72 | 6Q71 | 6Q70 |

*Values between parentheses correspond to the highest resolution shells.

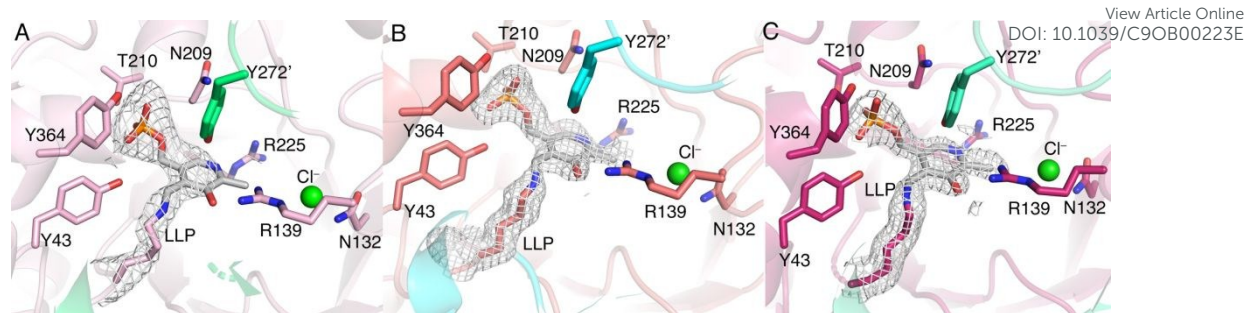
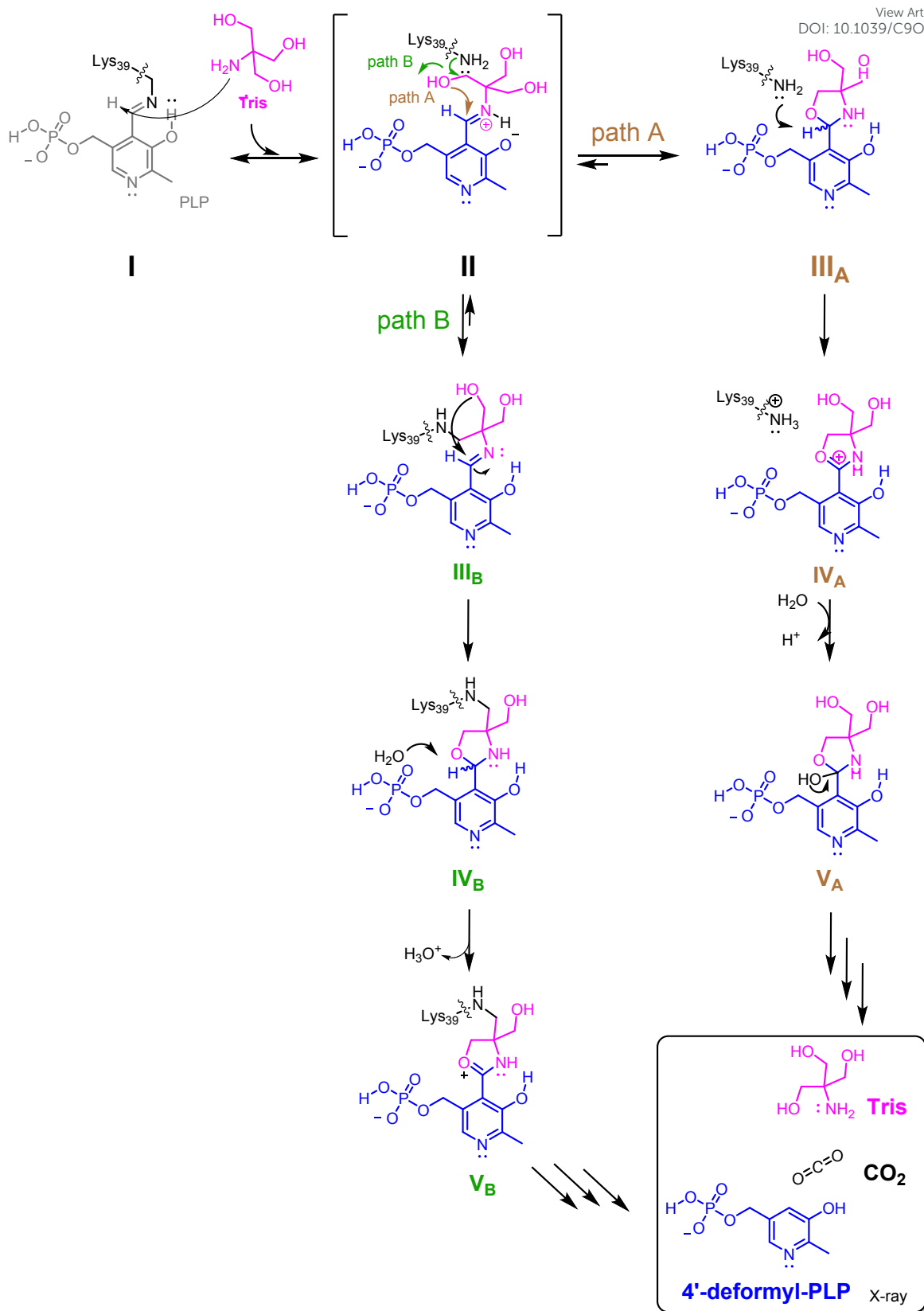


Figure 4. Electron density ($2F_o - F_c$ map contoured at 1σ) for of *BsAlaR* in the crystal structures obtained: (A) in the absence of buffer, (B) in the presence of bis-Tris propane pH 8.5, (C) in the presence of HEPES pH 8.5. Relevant residues and PLP cofactor depicted as capped sticks. Color codes as in Figure 1.

In light of these considerations, our unprecedented findings of internal aldimine bond cleavage and PLP degradation in a bacterial AlaR prompted us to search for a possible mechanism (**Scheme 2**). Electron density matching the size and shape of a Tris molecule from the buffer was found at the entrance to the active site, in the neighbourhood of Asp174/Asp174' and Tyr364/Tyr364' (**Figure 1B**). In common with natural α -amino acids, Tris contains a primary amine but, in contrast to them, it lacks a carboxylate group (**Figure 3**). Therefore, we reasoned that, rather than giving rise to the reversible reaction shown in **Scheme 1**,¹ the external aldimine formed by Tris might have evolved differently (**Scheme 2**) so as to eventually render the inactivated PLP cofactor and the free lysine observed in the X-ray crystal structure (**Figure 1**). In fact, earlier experimental work has already shown that the addition of Tris to a solution of PLP results in spectral changes consistent with formation of the corresponding Schiff base at high pH followed by evolution to a carbinolamine or addition of one of the three -OH groups of Tris to the double bond.¹⁴⁻¹⁶

Our mechanistic proposal (**Scheme 2**, path A) invokes an initial Tris-PLP adduct **III_A**, which can be deprotonated within the enzyme's active site to form the carbocation **IV_A**. The latter species, upon addition of a water molecule, would decompose to form **V_A**, which would finally evolve to Tris + CO₂ and 4'-deformyl-PLP, as observed in the X-ray crystal structure. As an alternative, and inspired by a hypothesis put forward to account for the inhibition of *h*BCATm by Tris [8], we also evaluated the possibility of generation of the double imine **III_B** before formation of the oxazolidine **IV_B** (**Scheme 2**, path B). Both reaction pathways were studied within the enzyme microenvironment by means of hybrid quantum mechanics / molecular mechanics (QM/MM) calculations [12].



Scheme 2. Proposed mechanism for the Tris-assisted 4'-deformylation of PLP in *BsAlaR*.

An expanded scheme can be found in **Figure S2** of the ESI.

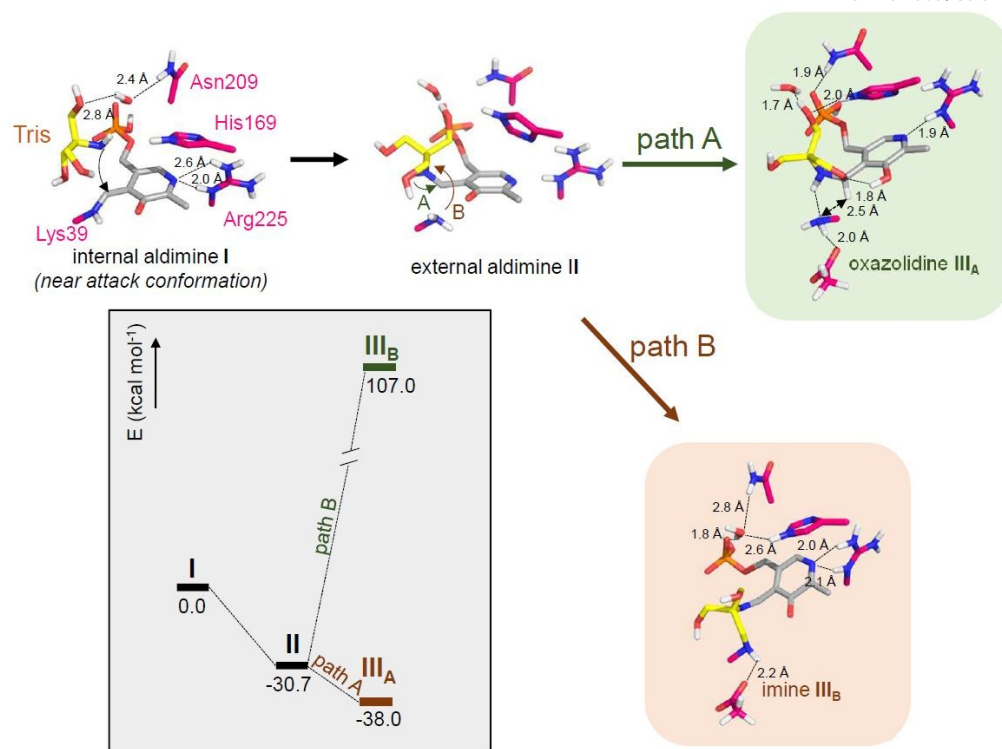


Figure 4. Detail of the geometries of the near-attack conformation **I** of Tris at the active site of *BsAlaR* and those of intermediates **III_A** (path A) and **III_B** (path B). The corresponding enthalpies (kcal mol⁻¹) computed at the B3LYP/6-31G(*d,p*) level of theory are shown in the grey box.

In the optimized near-attack conformation **I** (Figure 4), the deprotonated Tris (pK_a = 8.06 at 25 °C) is oriented within the active site of *BsAlaR* in a manner similar to that expected for its natural amino acid substrate, that is, with its attacking nitrogen close to C4'(PLP) (at 3.4 Å) and one of its hydroxyl groups mimicking one of the carboxylate oxygens. Once the trans-aldimination reaction occurs, the external aldimine **II** evolves to oxazolidine **III_A** in a process that is thermodynamically favourable ($\Delta E_{\text{II} \rightarrow \text{III}} = -7.2$ kcal mol⁻¹). In this regard, it is known that pyridyl-aldimines such as **II** are spontaneously converted (>95%) in solution to their corresponding 1,3-oxazolidines (e.g. **III_A**).^{17, 18} Besides, it has been demonstrated that the deprotonated form of the Tris-PLP Schiff base in highly alkaline solutions differs from analogous adducts of PLP with amino acids Gly or Val, for which a downshift of the absorption maximum and the appearance of the 4'-H signal in the ¹H-NMR spectrum at much lower chemical shift values (9.2 → 6.2 ppm) are observed. These pieces of evidence are indicative of the absence of an aldimine such as **II**.^{17, 18} Furthermore, the β-aminopolyol Tris has been used as a reagent for the synthesis of oxazolidines through condensation reactions

with ketones.¹⁹ The alternative intermediate **III_B** (pathway B, **Scheme 2**) seems unlikely due to the high energy of imine **III_B** (**Figure 3**). Besides, this path would require an additional hydrolysis step (**III_B** → **IV_B**) to reach the oxazolidine intermediate. Altogether, we propose that Tris may assist the deformylation of the cofactor by formation of oxazolidine **III_A** as an intermediate.

In contrast to the previous outcome in solution, and as a consequence of the chemical environment within the active site of *BsAlaR*, oxazolidine **III_A** may evolve to **IV_A** through a Lys39-assisted deprotonation (**Figure 4**). On the one hand, the acidity of H4' is increased by the hydrogen-bonding network involving oxazolidine O2; on the other hand, the attacking nitrogen of Lys39 is activated by the Asp321 carboxylate. The optimized geometry of oxazolidine **IV_A** is reminiscent of the structures of the external aldimine adducts formed by cycloserine-derived inhibitors within the active site of prokaryotic AlaR racemases²⁰ and *M. tuberculosis* BCAT.²¹ In the present case, however, C1 of Tris in **IV_A** cannot be protonated/deprotonated by Tyr272'/Lys39. Nonetheless, this highly electrophilic intermediate can be attacked by a proximal nucleophile, namely a water molecule. In fact, the crystallographic water molecule HOH¹⁵¹, which would be activated by Tyr272'/His169 and the phosphate group, can add onto C4' to form **V_A**. This hydroxylated intermediate would evolve to **VI_A** and 4'-deformylpyridoxal upon breakage of the C—C bond. Intermediate **V_A** is formally a masked 4-carboxy-3-hydroxypyridine that can decompose to CO₂ and 3-hydroxypyridine, in analogy to other pyridine carboxylates, through an assisted 1,3-dicarbonyl decarboxylation²² with the participation of a second water molecule.

It must be stressed that, despite its widespread use as a standard buffer component in biochemical and biophysical research, Tris can (i) degrade peptides such as substance P,²³ (ii) act on several proteins as a nucleophile,²⁴ and (iii) scavenge hydroxyl radicals.²⁵ Of even more relevance to our case, Tris has also been reported as an agent capable of reversing the modification of lysine residues by PLP, unless the resulting Schiff base is stabilized by reduction with NaBH₄.²⁶ In fact, some PLP-containing enzymes, such as tryptophanase,⁷ kynurenine-oxoglutarate transaminase (KAT),^{10, 27} threonine dehydratase and threonine deaminase,^{28, 29} are known to be inactivated in the presence of Tris-HCl buffer, the activity being restored only upon incubation with added PLP. In relation to these observations, it is known that freezing favours the trapping of intermediates accumulated during the steady state of the reaction in enzyme crystals.³⁰ In addition,

under these circumstances, high concentrations of organic cosolvents can also give rise to denaturation, change in ligand binding and altered enzyme-substrate interactions.³¹ We show here that something similar happens to *BsAlaR* in the presence of Tris and we rationalize this finding by proposing that intermediate **III_A** is generated after flash cooling. Taken together, our results highlight that Tris, a common buffer component, can act as a mechanism-based inactivator of a PLP-containing enzyme at subzero temperatures.

Experimental and computational procedures

Cloning and purification of *BsAlaR*.

The *Bacillus subtilis* gene *Bsu17640* encoding *BsAlaR* was cloned into the pET28b plasmid (Novagen) for expression in *E. coli* BL21(DE3) cells.³² Expression was induced (at OD₆₀₀ = 0.4) with 1 mM IPTG for 2 h. Cell pellets were resuspended in 50 mM Tris HCl pH 7.5, 150 mM NaCl and Complete Protease Inhibitor Cocktail Tablets (Roche), and lysed through a French press. Proteins were purified from cleared lysates (30 min; 65,000 rpm) on Ni-NTA agarose columns (Qiagen) and eluted with a discontinuous imidazole gradient. Pure proteins were visualized by SDS-PAGE.³³

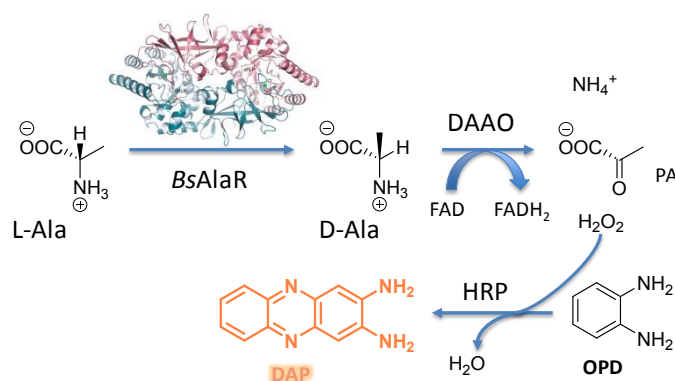


Figure 5. Scheme of the enzyme-coupled assay used to measure *BsAlaR* activity. DAAO, D-amino acid oxidase; HRP, horseradish peroxidase; OPD, *o*-phenylenediamine; DAP, 2,3-diaminophenazine; PA, pyruvate. The cartoon representation of homodimeric *BsAlaR* corresponds to PDB entry 5IRP.

Racemase activity assay.

An enzyme-coupled assay (**Figure 5**) was used to measure *BsAlaR* activity.³⁴ First, the enzyme was incubated in either Tris-HCl 100 mM at different pH values: 6.8, 7.5, 8.0, 8.8, and 9.0 or carbonate-bicarbonate buffer (pH 9.0). The reaction mixture was prepared with each specific buffer in a final volume of 50 μ L and catalysis was allowed to proceed for 30 s at room temperature using 0.57 μ M of *BsAlaR* and 20 mM of L-Ala as the substrate. The reaction was stopped by boiling for 10 min. The samples were then centrifuged for 10 minutes at 14,500 rpm to remove the inactivated protein and the reaction product was mixed with D-amino acid oxidase, an FAD-containing flavoenzyme that catalyzes the oxidative deamination of D-Ala to its corresponding α -keto acid (*i.e.* pyruvic acid), ammonium and hydrogen peroxide. H_2O_2 is then reduced to water by horseradish peroxidase and *o*-phenylenediamine is simultaneously oxidized to give the chromogenic 2,3-diaminophenazine.³⁵ The specific activity was determined by measuring, in triplicates, the production rate for 20 mM of L-Ala at different time points (0.5–5 min). The specific activity was calculated as μ g of L-Ala racemized per min and per amount of enzyme.

Crystallization of *BsAlaR*. Crystals of *BsAlaR* were obtained by the hanging drop method in four different crystallization conditions: (a) 15% PEG 4000, 0.2 M $MgCl_2$ (*BsAlaR*–nobuff), 0.1 M Tris pH = 8.5; (b) 15% PEG 4000, 0.2 M $MgCl_2$ (*BsAlaR*–TRS); (c) 13% PEG 4000, 0.2 M $MgCl_2$, bis-TRIS propane pH=8.5 (*BsAlaR*–TRSprop); and (d) 15% PEG 4000, 0.2 M $MgCl_2$, 0.1 M HEPES pH = 8.5 (*BsAlaR*–HEPES) at a concentration of 3.5 mg/mL. Drops containing 1 μ L of protein with 1 μ L of reservoir solution were equilibrated against 150 μ L of reservoir solution. The optimized crystallization conditions were obtained using the microbatch technique. X-ray data sets were

collected from flash-cooled crystals at 100 K. Before cooling, the crystals were washed for a few seconds in a cryoprotectant solution of 70% (v/v) Paratone.

X-ray data collection and structural determination. The X-ray diffraction data set from *BsAlaR*–TRS was collected on beamline ID23-1 at ESRF (Grenoble, France) with 1° oscillation between images and up to 2.1 Å resolution. The remaining datasets were collected on beamline XALOC at ALBA (Barcelona, Spain) with 0.25° oscillation range for *BsAlaR*–nobuff and 0.2° for both *BsAlaR*–TRSProp and *BsAlaR*–HEPES. *BsAlaR*–nobuff, *BsAlaR*–TRSProp and *BsAlaR*–HEPES diffracted up to 2.85 Å, 1.95 Å, and 2.05 Å, respectively (**Table 1**). The data sets were processed using iMOSFLM³⁶ and XDS³⁷, and were scaled with AIMLESS from the CCP4³⁸ program suite.

The *BsAlaR*–TRS structure was solved by the molecular replacement method using MOLREP³⁹ and *Bacillus anthracis* AlaR (PDB code 3HA1) as the template. The model was completed manually using Coot⁴⁰. *BsAlaR*–TRSProp and *BsAlaR*–HEPES were solved using as template the *BsAlaR*–TRS structure obtained previously. *BsAlaR*–TRS R_{work} converged to 0.16 and the R_{free} to 0.20 in the final model, *BsAlaR*–nobuff R_{work} 0.20 and R_{free} 0.25, *BsAlaR*–TRSProp R_{work} 0.20 and R_{free} to 0.23, *BsAlaR*–HEPES R_{work} 0.19 and R_{free} 0.24. The coordinates were refined using Phenix⁴¹ and Refmac from the CCP4³⁸ program suite and modelled using Coot.⁴⁰ The data refinement results are summarized in **Table 1**.

Molecular dynamics (MD) simulations. The initial geometry was prepared using the *BsAlaR*

coordinates (PDB id. 5IRP) and replacing the decarboxylated PLP by a full-reconstituted Lys39-PLP internal aldimine and a free neutral Tris molecule. Before running the mechanistic studies, a restrained MD simulation protocol was followed. The enzyme was immersed in a cubic box of 12 Å from the solute to the border of the box filled with *ca.* 24,500 TIP3P water molecules⁴² and 17 chloride ions to ensure electroneutrality. The *tleap* utility in AMBER14⁴³ was used for the setup of all systems. Periodic boundary conditions were used and the electrostatic interactions were computed using the Ewald method⁴⁴ with a grid spacing of 1 Å. The cutoff distance for the non-bonded interactions was 10 Å and the SHAKE algorithm⁴⁵ was applied to all bonds involving hydrogens. An integration step of 2.0 fs was defined. Before the production phase, the energy of each simulated system was minimized sequentially in three steps: initially only the hydrogens, then the waters plus the counterions, and finally the whole molecular ensemble, in every case by first using the steepest descendent algorithm and then the conjugate gradient method. The resulting energy-minimized solvated geometries were heated from 100 to 300 K over 100 ps using the Berendsen thermostat but keeping the positions of all the heavy atoms of the solute restrained with a harmonic constant of 20 kcal⁻¹ mol⁻¹ Å⁻²; in this step, a random seed was imposed. Thereafter, the imposed restraints were gradually removed in 5 steps of 20 ps each, during which the system was switched from an NVT (40 to 10 kcal⁻¹ mol⁻¹ Å⁻² in 80 ps, constant volume) to an NPT (10 kcal⁻¹ mol⁻¹ Å⁻² in 40 ps, constant pressure) ensemble. Throughout this procedure, we could identify an initial optimized geometry for the QM/MM MD studies. All the MD simulations were carried out using the *pmemd.cuda_SPFP* module from the AMBER14⁴³ suite of programs running on a GPU architecture (NVIDIA GeForce GTX980). System build-up, distance monitoring and cluster analysis were carried out using the *cpptraj* module in AMBER14.⁴⁶

Hybrid quantum mechanics / molecular mechanics (QM/MM) MD studies. The QM region was defined so as to include the PLP cofactor, the active-site Tris molecule and the side chains of the following relevant *BsAlaR* amino acids: (i) catalytic residues Lys39 and Tyr272' and their assisting partners Asp321 and His169; (ii) PLP-anchoring residues Tyr43, Tyr364, Arg225, Arg139; and (iii) the proximal Asn209. In addition, the crystallographic water molecule HOH¹⁵¹ and a second water molecule (WAT_B), as defined in our mechanistic proposal, were also included. All the QM/MM MD reaction pathways were simulated for 10 ps making use of the SCC-DFTB:leaprc.14SB method⁴⁷ in AMBER14. The initial near-attack conformation and all intermediates were energy minimized before/after the simulation of the reactions by means a QM/MM MD protocol (DFTB:leaprc.14SB, 20,000 cycles). Finally, the geometries of the QM regions of the resulting complexes were optimized at a higher level of theory using the cluster method.

Cluster method (QM optimizations). The same QM region defined above but including the side chain of Asn209 was used for the definition of the QM region. The resulting geometry obtained after the QM/MM MD simulation was optimized at the DFT level of theory using the hybrid functional B3LYP and the 6-31G(*d,p*) basis set but the heavy atoms were kept frozen to preserve the conformation found in the protein. All the energies were computed including the zero-point energy correction. All the optimizations were run using program Gaussian09, revision D.01.⁴⁸ The cartesian coordinates of the optimized geometries of the complexes shown in Scheme 2 can be found in the ESI file Structures.xyz.

Conflicts of interest

There are no conflicts of interest to declare.

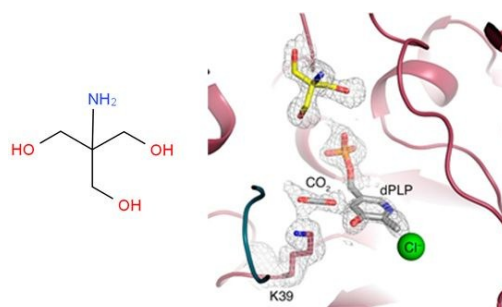
View Article Online
DOI: 10.1039/C9OB00223E

Acknowledgments

Financial support from the Spanish Ministry of Science and Innovation to F.G. (SAF2015-64629-C2-2-R) and J.A.H. (BFU2017-90030-P) is gratefully acknowledged. F. Cava is supported by the Laboratory for Infection Medicine Sweden (MIMS), the Knut and Alice Wallenberg Foundation (KAW), and the Swedish Research Council. We thank the staff at ESRF and ALBA synchrotron radiation facilities for support in data collection. We are grateful to Alberto Mills (UAH) for valuable help in artwork preparation.

Keywords: Tris • pyridoxal 5'-phosphate • racemase • X-ray crystallography • molecular modelling

TOC graphic



The commonly used Tris buffer acts as a surrogate substrate and deformylates pyridoxal phosphate in a bacterial alanine racemase at subzero temperatures.

Notes and references

- 1 N. Bernardo-García, P. Sánchez-Murcia, F. Gago, F. Cava and J. A. Hermoso, *Curr. Org. Chem.*, 2016, **20**, 1222-1231.
- 2 A. C. Eliot and J. F. Kirsch, *Annu. Rev. Biochem.*, 2004, **73**, 383-415.
- 3 H. Im, M. L. Sharpe, U. Strych, M. Davlieva and K. L. Krause, *BMC Microbiol.*, 2011, **11**, 116.
- 4 A. Espaillat, C. Carrasco-López, N. Bernardo-García, N. Pietrosevoli, L. H. Otero, L. Alvarez, M. A. de Pedro, F. Pazos, B. M. Davis, M. K. Waldor, J. A. Hermoso and F. Cava, *Acta Crystallogr. Sect. D. Biol. Crystallogr.*, 2014, **70**, 79-90.
- 5 P. E. Bock and C. Frieden, *Trends Biochem. Sci.*, 1978, **3**, 100-103.
- 6 T. Erez, G. Y. Gdalevsky, C. Hariharan, D. Pines, E. Pines, R. S. Phillips, R. Cohen-Luria and A. H. Parola, *Biochim. Biophys. Acta*, 2002, **1594**, 335-340.
- 7 K. P. Gopinathan and R. D. DeMoss, *Biochemistry*, 1968, **7**, 1685-1691.
- 8 A. Kogan, G. Y. Gdalevsky, R. Cohen-Luria, Y. Goldgur, R. S. Phillips, A. H. Parola and O. Almog, *BMC Struct. Biol.*, 2009, **9**, 65.
- 9 M. N. Isupov, A. A. Antson, E. J. Dodson, G. G. Dodson, I. S. Dementieva, L. N. Zakomirdina, K. S. Wilson, Z. Dauter, A. A. Lebedev and E. H. Harutyunyan, *J. Mol. Biol.*, 1998, **276**, 603-623.
- 10 Q. Han, H. Robinson, T. Cai, D. A. Tagle and J. Li, *J. Med. Chem.*, 2009, **52**, 2786-2793.
- 11 N. Yennawar, J. Dunbar, M. Conway, S. Hutson and G. Farber, *Acta Crystallogr. Sect. D. Biol. Crystallogr.*, 2001, **57**, 506-515.
- 12 S. Rety, P. Deschamps and N. Leulliot, *Acta Crystallogr. Sect. D: Biol. Crystallogr.*, 2015, **71**, 1378-1383.
- 13 E. V. Filippova, G. Minasov, K. Flores, H. V. Le, R. B. Silverman, R. L. McLeod and W. F. Anderson, (*unpublished*), 2015, DOI: 10.2210/pdb5EQC/pdb.
- 14 M. D. Davis, D. E. Edmondson and D. B. McCormick, *Monatsh. Chem.*, 1982, **113**, 999-1004.
- 15 Y. Kobayashi and K. Makino, *Biochim. Biophys. Acta*, 1970, **208**, 137-140.
- 16 J. Mitra and D. E. Metzler, *Biochim. Biophys. Acta*, 1988, **965**, 93-96.
- 17 S. Barman, K. L. Diehl and E. V. Anslyn, *RSC Adv.*, 2014, **4**, 28893.
- 18 R. F. Martínez, M. Ávalos, R. Babiano, P. Cintas, J. L. Jiménez, M. E. Light, J. C. Palacios and E. M. S. Pérez, *Eur. J. Org. Chem.*, 2010, **2010**, 6224-6232.
- 19 M. Darabantu, G. Plé, C. Maieranu, I. Silaghi-Dumitrescu, Y. Ramondenc and S. Mager, *Tetrahedron*, 2000, **56**, 3799-3816.
- 20 T. D. Fenn, G. F. Stamper, A. A. Morollo and D. Ringe, *Biochemistry*, 2003, **42**, 5775-5783.
- 21 T. M. Amorim Franco, L. Favrot, O. Vergnolle and J. S. Blanchard, *ACS Chem. Biol.*, 2017, **12**, 1235-1244.
- 22 D. Palm, A. A. Smucker and E. E. Snell, *J. Org. Chem.*, 1967, **32**, 826-828.
- 23 T. Higa and D. M. Desiderio, *Anal. Biochem.*, 1988, **173**, 463-468.
- 24 R. L. Lundblad, *Chemical reagents for protein modification*, CRC Press, Taylor & Francis Group, Boca Raton, 4th edn., 2014.
- 25 M. Hicks and J. M. Gebicki, *FEBS Lett.*, 1986, **199**, 92-94.
- 26 H. Nishigori and D. Toft, *J. Biol. Chem.*, 1979, **254**, 9155-9161.
- 27 D. Schomburg and D. Stephan, in *Enzyme Handbook 13 - Class 2.5 - EC 2.7.1.104 Transferases* eds. D. Schomburg and D. Stephan, 1997, DOI: 10.1007/978-3-642-59176-1, ch. Kynurenine-oxoglutarate transaminase, pp. 235-238.

- 28 H. G. Ghazarian and R. Borchers, *Proc. Soc. Exp. Biol. Med.*, 1972, **139**, 113-114.
- 29 G. W. Hatfield and H. E. Umbarger, *J. Biol. Chem.*, 1970, **245**, 1736-1741.
- 30 I. T. Weber, J. Agniswamy, G. Fu, C.-H. Shen and R. W. Harrison, 2012, **87**, 57-86.
- 31 M. W. Makinen and A. L. Fink, *Annu. Rev. Biophys. Bioeng.*, 1977, **6**, 301-343.
- 32 A. H. Rosenberg, B. N. Lade, D. S. Chui, S. W. Lin, J. J. Dunn and F. W. Studier, *Gene*, 1987, **56**, 125-135.
- 33 U. K. Laemmli and M. Favre, *J. Mol. Biol.*, 1973, **80**, 575-599.
- 34 E. Rosini, L. Caldinelli and L. Piubelli, *Front Mol Biosci*, 2017, **4**, 102.
- 35 A. Espaillet, C. Carrasco-Lopez, N. Bernardo-Garcia, N. Pietrosevoli, L. H. Otero, L. Alvarez, M. A. de Pedro, F. Pazos, B. M. Davis, M. K. Waldor, J. A. Hermoso and F. Cava, *Acta Crystallogr D Biol Crystallogr*, 2014, **70**, 79-90.
- 36 T. G. Battye, L. Kontogiannis, O. Johnson, H. R. Powell and A. G. Leslie, *Acta Crystallogr D Biol Crystallogr*, 2011, **67**, 271-281.
- 37 W. Kabsch, *Acta Crystallogr D Biol Crystallogr*, 1988, **66**, 125-132.
- 38 M. D. Winn, C. C. Ballard, K. D. Cowtan, E. J. Dodson, P. Emsley, P. R. Evans, R. M. Keegan, E. B. Krissinel, A. G. W. Leslie, A. McCoy, S. J. McNicholas, G. N. Murshudov, N. S. Pannu, E. A. Potterton, H. R. Powell, R. J. Read, A. Vagin and K. S. Wilson, *Acta Crystallogr. Sect. D. Biol. Crystallogr.*, 2011, **67**, 235-242.
- 39 A. Vagin and A. Teplyakov, *Acta Crystallogr D Biol Crystallogr*, 2010, **66**, 22-25.
- 40 P. Emsley, B. Lohkamp, W. G. Scott and K. Cowtan, *Acta Crystallogr. Sect. D. Biol. Crystallogr.*, 2010, **66**, 486-501.
- 41 P. V. Afonine, R. W. Grosse-Kunstleve, N. Echols, J. J. Headd, N. W. Moriarty, M. Mustyakimov, T. C. Terwilliger, A. Urzhumtsev, P. H. Zwart and P. D. Adams, *Acta Crystallogr. Sect. D. Biol. Crystallogr.*, 2012, **68**, 352-367.
- 42 J. Wang, R. M. Wolf, J. W. Caldwell, P. A. Kollman and D. A. Case, *J. Comput. Chem.*, 2004, **25**, 1157-1174.
- 43 D. A. Case, V. Babin, J. Berryman, R. M. Betz, Q. Cai, D. S. Cerutti, T. E. Cheatham III, T. A. Darden, R. E. Duke, H. Gohlke, A. W. Goetz, S. Gusarov, N. Homeyer, P. Janowski, J. Kaus, I. Kolossvary, A. Kovalenko, T. S. Lee, S. LeGrand, T. Luchko, R. Luo, B. Madej, K. M. Merz, F. Paesani, D. R. Roe, A. Roitberg, C. Sagui, R. Salomon-Ferrer, G. Seabra, C. L. Simmerling, W. Smith, J. Swails, R. C. Walker, J. Wang, R. M. Wolf, X. Wu and P. A. Kollman, *AMBER 14*, University of California, San Francisco, 2014.
- 44 P. F. Batcho, D. A. Case and T. Schlick, *J. Chem. Phys.*, 2001, **115**, 4003-4018.
- 45 J.-P. Ryckaert, G. Ciccotti and H. J. C. Berendsen, *J. Comput. Phys.*, 1977, **23**, 327-341.
- 46 D. R. Roe and T. E. Cheatham, 3rd, *J. Chem. Theory Comput.*, 2013, **9**, 3084-3095.
- 47 G. d. M. Seabra, R. C. Walker, M. Elstner, D. A. Case and A. E. Roitberg, *J. Phys. Chem. A*, 2007, **111**, 5655-5664.
- 48 M. J. Frisch, G. W. Trucks, H. B. Schlegel, G. E. Scuseria, M. A. Robb, J. R. Cheeseman, G. Scalmani, V. Barone, B. Mennucci, G. A. Petersson, H. Nakatsuji, M. Caricato, X. Li, H. P. Hratchian, A. F. Izmaylov, J. Bloino, G. Zheng, J. L. Sonnenberg, M. Hada, M. Ehara, K. Toyota, R. Fukuda, J. Hasegawa, M. Ishida, T. Nakajima, Y. Honda, O. Kitao, H. Nakai, T. Vreven, J. A. Montgomery Jr., J. E. Peralta, F. Ogliaro, M. J. Bearpark, J. Heyd, E. N. Brothers, K. N. Kudin, V. N. Staroverov, R. Kobayashi, J. Normand, K. Raghavachari, A. P. Rendell, J. C. Burant, S. S. Iyengar, J. Tomasi, M. Cossi, N. Rega, N. J. Millam, M. Klene, J. E. Knox, J. B. Cross, V. Bakken,

View Article Online
DOI: 10.1039/C9OB00223E

C. Adamo, J. Jaramillo, R. Gomperts, R. E. Stratmann, O. Yazyev, A. J. Austin, R. Cammi, C. Pomelli, J. W. Ochterski, R. L. Martin, K. Morokuma, V. G. Zakrzewski, G. A. Voth, P. Salvador, J. J. Dannenberg, S. Dapprich, A. D. Daniels, Ö. Farkas, J. B. Foresman, J. V. Ortiz, J. Cioslowski and D. J. Fox, *Gaussian 09*, Gaussian, Inc., Wallingford, CT, USA, A.01 edn., 2009.

[View Article Online](#)
DOI: 10.1039/C9OB00223E

Footnote

† Electronic supplementary information (ESI) available: Full reaction scheme and additional crystallographic data.